

Physical and dynamical characterisation of low ΔV NEA (190491) 2000 FJ₁₀^{*}

A. A. Christou¹, T. Kwiatkowski², M. Butkiewicz², A. Gulbis³, C. W. Hergenrother⁴, S. Duddy⁵, and A. Fitzsimmons⁶

¹ Armagh Observatory, College Hill, Armagh BT61 9DG, UK e-mail: aac@arm.ac.uk

² Astronomical Observatory Institute, Faculty of Physics, A. Mickiewicz University, Słoneczna 36, 60-286 Poznań, Poland

³ Southern African Large Telescope and South African Astronomical Observatory, Observatory Road, Observatory, 7925, South Africa

⁴ Lunar and Planetary Laboratory, University of Arizona, Tucson AZ 85721-0092, USA

⁵ Centre for Astrophysics and Planetary Science, School of Physical Sciences, University of Kent, Canterbury CT2 7NH, UK

⁶ Astrophysics Research Centre, School of Mathematics and Physics, Queen's University Belfast, Belfast BT7 1NN, UK

Received 02 Aug 2012 / Accepted Oct 2012

ABSTRACT

Aims. We investigated the physical properties and dynamical evolution of Near Earth Asteroid (NEA) (190491) 2000 FJ₁₀ in order to assess the suitability of this accessible NEA as a space mission target.

Methods. Photometry and colour determination were carried out with the 1.54 m Kuiper Telescope (Mt Bigelow, USA) and the 10 m Southern African Large Telescope (SALT; Sutherland, South Africa) during the object's recent favourable apparition in 2011-12. During the earlier 2008 apparition, a spectrum of the object in the 6000-9000 Angstrom region was obtained with the 4.2 m William Herschel Telescope (WHT; Canary IIs, Spain). Interpretation of the observational results was aided by numerical simulations of 1000 dynamical clones of 2000 FJ₁₀ up to 10⁶ yr in the past and in the future.

Results. The asteroid's spectrum and colours determined by our observations suggest a taxonomic classification within the S-complex although other classifications (V, D, E, M, P) cannot be ruled out. On this evidence, it is unlikely to be a primitive, relatively unaltered remnant from the early history of the solar system and thus a low priority target for robotic sample return. Our photometry placed a lower bound of 2 hrs to the asteroid's rotation period. Its absolute magnitude was estimated to be 21.54 ± 0.1 which, for a typical S-complex albedo, translates into a diameter of 130 ± 20 m. Our dynamical simulations show that it has likely been an Amor for the past 10⁵ yr. Although currently not Earth-crossing, it will likely become so during the period 50 – 100 kyr in the future. It may have arrived from the inner or central Main Belt > 1 Myr ago as a former member of a low-inclination S-class asteroid family. Its relatively slow rotation and large size make it a suitable destination for a human mission. We show that ballistic Earth-190491-Earth transfer trajectories with $\Delta V < 2 \text{ km s}^{-1}$ at the asteroid exist between 2052 and 2061.

Key words. Minor planets, asteroids: individual: 2000 FJ₁₀ - Methods: observational - Methods: numerical

1. Introduction

The population of near-Earth asteroids (NEAs) contains a small fraction of objects in low inclination, low-eccentricity orbits similar to the Earth's. These NEAs are considered attractive targets for in situ investigation by robots or humans (Hasegawa et al. 2008; Abell et al. 2009; Michel et al. 2009; Lauretta et al. 2010; Elvis et al. 2011). However, the attractiveness of individual objects as targets for either robotic or human missions is mired by the currently poor knowledge of their orbits and physical properties. Many have been observed only on a single apparition resulting in large projected uncertainties in their future position. In addition, knowledge of properties that are important from an operational as well as a scientific standpoint -

size, shape, surface roughness, rotational state and spectral type - ranges from poor to non-existent. Part of the problem stems from their Earth-like orbits; slow keplerian shear generally places them beyond the reach of Earth-based observatories except during the few months that they spend in proximity to the Earth every decade or so. The situation is also not helped by their small sizes, typically a few tens of metres, so even when near the Earth their study is the exclusive purview of large-aperture instruments. Primitive NEA taxonomies - those belonging to classes B, C, D, and P - are preferred as mission targets for robotic sample return as they are thought to be relatively unaltered relics of the early solar system (eg Michel et al. 2009). In addition, fast rotators are unsuitable as mission targets due to the added complexity of operations in close proximity to such objects.

^{*} based on observations made with the Southern African Large Telescope (SALT)

This paper reports on a study of NEA (190491) 2000 FJ₁₀, an object that is accessible from the Earth (Section 2). A programme of observations of 190491 was carried out with the 4.2 m William Herschel Telescope (WHT), the 10 m Southern African Large Telescope (SALT) and the 1.5 m Kuiper telescope (Section 3) aiming to constrain its taxonomic type, size, and rotational state (Section 4). Those were combined with numerical simulations of 190491's orbital evolution (Section 5) to provide context for the observational characterisation and help us draw conclusions on the object's likely origin (Section 6). Its accessibility from the Earth was quantified by constructing direct, two-way keplerian trajectories between the Earth and the asteroid (Section 7). A summary of our findings is provided in Section 8.

2. The Asteroid

(190491) 2000 FJ₁₀ was discovered by the Spacewatch survey on 25 March 2000. Based on its orbital parameters ($a = 1.32$ AU, $e = 0.23$, $i = 5^\circ$) it is classified as an Amor Near Earth Asteroid (NEA). Its absolute magnitude $H = 20.9$ implies a diameter ranging from 110–390 m for an albedo range 0.05–0.5. Its Earth Minimum Orbit Intersection Distance (MOID) is 0.055 AU, slightly higher than the threshold of 0.05 AU for classifying it as a Potentially Hazardous Asteroid (PHA). It is one of the most accessible spacecraft targets, ranking 124th out of 8857 object entries in the list of Near Earth Asteroid ΔV for spacecraft rendezvous¹ as of May 2012. Its ΔV as stated in that list is 4.567 km s^{-1} , slightly above the threshold that would classify it an Ultra Low Delta V (ULDV) object (Elvis et al. 2011). However, its absolute magnitude is the second-brightest within those objects that precede it, the first being the ULDV NEO (89136) 2001 US16 with $H = 20.2$ and $\Delta V = 4.428 \text{ km s}^{-1}$.

3. Observations and Data reduction

3.1. SALT

Located at SAAO in South Africa, the 10 m SALT is based on the Hobby-Eberly Telescope (Texas, USA) with a payload moving during the observations above the stationary 10 m spherical mirror (Kwiatkowski et al. 2010, and references therein). It can access objects in the declination range from $\delta = -75^\circ$ to $\delta = +10^\circ$ when they enter the annular region on the sky located between zenith distances from 48° to 59° . SALT works solely in the queue-scheduling mode, in which the exact time of the observations is not known in advance.

Because of its construction, during observations the telescope's pupil continuously changes making it impossible to perform all-sky photometry. For the same reason, twilight flat fields cannot be used in the photometric reduction. Instead, night sky flat fields derived directly from the science frames have to be used.

We observed 2000 FJ₁₀ with SALT during September 2011, on the first month of the facility's normal operation after an extended period of commissioning. The instrument of choice was the SALT imaging camera (SALTICAM;

O'Donogue et al. 2003), a mosaic of two CCDs, each with two readout amplifiers.

The aspect data and the observing log are provided in Table 1. During that period the asteroid was located within a star field covered by the Sloan Digital Sky Survey (hereafter SDSS), which allowed us to calibrate our photometry with SDSS standard stars. Under normal operations (the case for the observations reported here), there is an effort to keep target and comparison sources on the same chip so as to ease data analysis. This limited our Field of View (hereafter FoV) but still left us with enough SDSS stars for comparison.

In order to determine colour indices we used the Sloan g , r and i filters. Because of the significant fringing in the infrared, the z filter was not used. As the lower bound of the range of the possible effective diameters of 2000 FJ₁₀ was 110 m, its rotation period could be as short as 10 min (eg Hergenrother & Whiteley 2011). To check that, the first run on 15 Sep, which lasted 20 min, was done with the r filter only. A preliminary reduction showed all photometric data points to be within the ± 0.05 mag range. The next run on 22 Sep lasted 50 min. It was executed with all three filters, in the following sequence: $10 \times r$, $3 \times g$, r , $3 \times g$, r , $3 \times g$, r , $3 \times i$, r , $3 \times i$. Sequencing the observations in this way allowed us to use r exposures to search for brightness variations, and – if necessary – reduce the magnitudes obtained in the other two filters to the same reference level.

Data reduction was done in two stages. First, the CCD frames were corrected for cross-talk and bias using the specialised PySALT package (Crawford et al. 2010). Next, following Kniazev & Vaisanen (2011), a flat-field correction was carried out using night sky flat-fields obtained from the science frames themselves.

An illumination pattern for each frame was created by removing the stars with a median filter and fitting a polynomial to the remaining background sky. The original frames were then divided by these flat-fields. During the observations the telescope was dithered every 3 exposures so that the stars did not occupy the same positions within the FoV. This allowed us to use all frames in a given filter – already corrected for the low frequency pattern – to produce a global, second-stage flat-field by median combining the images. The obtained flat-field mapped the constant pixel-to-pixel variations within the FoV. Finally, all images in a given filter were divided by the global flat-field frame.

The instrumental magnitudes of the SDSS stars and of the asteroid were then measured with standard aperture photometry. Both the flat-field corrections and the photometry were done with the STARLINK package, maintained at the Joint Astronomy Centre of Mauna Kea Observatory.

A problem in calibrating the instrumental magnitudes to the SDSS standard scale was the unknown transformation between the photometric systems of SALT and SDSS. While this would require a detailed analysis, we instead performed a simple, first-order check with the available data, obtained through the SALT g_S , r_S , and i_S filters. It revealed some linear trends of $r_S - r$ vs. $r - g$, $g_S - g$ vs. $r - g$, $i_S - i$ vs. $g - i$, which led to ≈ 0.04 mag differences between red and blue stars. Because of this fact, for determination of asteroid colours we selected only the solar type SDSS stars (having $0.4 < g - r < 0.5$ mag and $0.1 < r - i < 0.2$ mag), for which the discrepancies between both SALT and SDSS photometric systems could be neglected. The asteroid magnitudes in each filter were mea-

¹ http://echo.jpl.nasa.gov/~lance/delta_v/delta_v.rendezvous.html

sured with respect to 3-4 SDSS solar colour stars, and the results were averaged. This way the uncertainties of the SDSS catalogue were minimised.

On 22 Sep, during 47 minutes, the brightness of the asteroid, as monitored in our *r* filter exposures, did not show any systematic changes. This allowed us to average the measurements, obtained in *r*, *g*, and *i* filters, and use them to compute colour indices. The obtained results are: $g - r = 0.59 \pm 0.03$ mag, $r - i = 0.21 \pm 0.03$ mag.

3.2. Kuiper telescope

The University of Arizona Kuiper 1.54-m telescope located near Mount Bigelow in southeastern Arizona was used to obtain V- and R-band photometry of 2000 FJ₁₀ on 9 separate dates between September 2011 and March 2012 (Table 1). On all 9 nights the asteroid was observed in the R-band. On the night of 2011 October 19 the asteroid was also observed in the V-band in order to measure its V-R color. The instrument used was the Mont4K, a Fairchild CCD486 4096 × 4097 CCD, with a FoV of $9'5 \times 9'5$ and plate scale of $0.28''/\text{pixel}$ when binned 2×2 .

All data were reduced with the IRAF software package. The images were bias-subtracted and flat-fielded with twilight and night sky flat images using the CCDRED package. The APPHOT package was used to perform aperture photometry of the asteroid and photometric standard stars. In order to compensate for variable seeing, the average *FWHM* was measured for each image and the photometric aperture was set to a radius of $2 \times FWHM$. Sky background was measured with a circular ring aperture of radius 20 pixels and width of 10 pixels. The sky aperture was centered on the position of the measured source. The telescope was tracked at the rate of motion of the asteroid and the images were shifted and co-added on the motion of the asteroid.

Photometric V- and R-band reference stars from Landolt (1992) were observed at multiple airmasses on each night in order to determine the photometric zero point and extinction coefficient.

The V- and R-band images were taken in the following sequence: $5 \times R$, $5 \times V$, $5 \times R$, $5 \times V$, $5 \times R$ and $5 \times V$. A V-R color index of 0.48 ± 0.05 mag was derived from the data. The cadence allowed for variability due to the rotation of the asteroid to be corrected. During the 37 minutes of observations, the asteroid steadily increased in brightness by ~ 0.3 magnitudes.

3.3. WHT

Observations were conducted using the Intermediate-dispersion Spectrograph and Imaging System (ISIS) mounted on the 4.2m William Herschel Telescope, La Palma (Table 1). Light from the optical system was split using the 5300 dichroic (blue cut off/red cut on at 5300 Angstroms) and directed along the red arm of the instrument. The red arm uses a red-sensitive $4k \times 2k$ pixel RED+ CCD with anti-reflection coating. The R158R grating with a slit width of 1 arcsecond were used producing a dispersion of 1.8 Angstroms per pixel. The total usable wavelength coverage from the red arm was 5300 to 10000 Angstroms, however the S/N degrades rapidly beyond 9000 Angstroms.

To ensure the NEA remained within the slit, non-sidereal tracking was used with the telescope tracking at

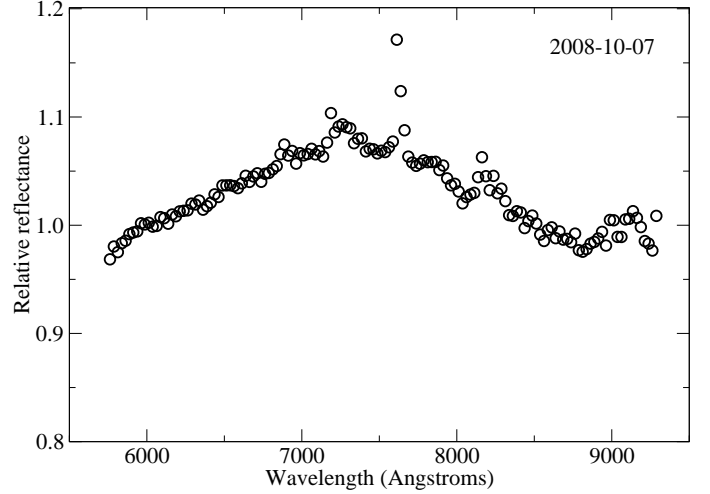


Fig. 1. Reflectance spectrum of (190491) 2000 FJ₁₀ obtained with the WHT. It is similar to the spectra of S type asteroids in the SMASS database.

the apparent rate of motion of the NEO. The position of the NEO was monitored throughout each exposure with manual corrections to the pointing position applied when necessary. In total $1 \times 600s + 3 \times 900s$ exposures were obtained.

Image reduction was performed in the usual manner. Bias images were combined and subtracted from the science images. Flat fielding was conducted after removal of the spectral profile of the tungsten lamp used to obtain the flat field images. The spectra were extracted using the IRAF task *apall*. Optimal extraction (Horne 1986) was used to improve the S/N of the extracted spectrum. Wavelength calibration was achieved using CuAr-CuNe arc lamp spectra observed at the same pointing position to account for the effects of flexure. The solar analog 16 Cyg B was observed to enable the removal of the solar spectrum from the NEA spectrum. Atmospheric correction was performed using tabulated extinction functions for La Palma (King 1985). These curves were scaled to the airmass of the observations of the NEA and solar analog and the corrections applied to each spectrum. Asteroid (1) Ceres was also observed and the spectrum extracted in this manner was consistent with previously published spectra (e.g Bus & Binzel 2002). Spectra were normalized and the solar spectrum removed. The result for 2000 FJ₁₀ is shown in Fig. 1.

Chi-squared fitting to the Bus-DeMeo taxonomy (DeMeo et al. 2009) was conducted. The spectra were re-sampled to produce reflectances at the wavelengths used to define the various taxonomic types. The best fit was to an Sq-type, but we note that the 1 micron absorption band has not been fully sampled, making a formal definition difficult.

4. Physical characteristics

4.1. Rotation period

As already explained, the specific construction of SALT limits its typical continuous observing run to 1 hour. Because of this, it is difficult to measure brightness variations with periods of several hours or longer. In the case of 2000 FJ₁₀ there was some possibility that – due to its small size – it is a fast rotator, with a rotation period $\ll 2$ hr. Fig. 2

Table 1. Aspect data and observing log

Date YYYY-MM-DD	Obs. time (UTC)	r [AU]	Δ [AU]	α [°]	λ [°]	β [°]	V [mag]	Mov ["/min]	Exp [s]	Filter	Telescope
2008-10-08	04:50 – 05:47	1.072	0.081	26.2	42.1	-8.8	16.7	4.3	$1 \times 600 +$ 3×900	Spec	WHT
2011-09-15	19:16 – 19:35	1.1674	0.1799	24.0	327.2	12.5	18.7	1.5	60	r	SALT
2011-09-22	21:23 – 22:13	1.1432	0.1680	31.4	324.2	9.6	18.7	1.5	60	g, r, i	SALT
2011-09-26	03:56 – 04:08	1.1325	0.1636	35.0	323.1	8.0	18.7	1.5	60	R	Kuiper
2011-10-19	03:40 – 04:17	1.0654	0.1441	57.9	320.7	-5.7	18.9	1.6	60	V, R	Kuiper
2011-10-21	03:35 – 03:46	1.0605	0.1429	59.5	321.0	-7.1	19.0	1.7	60	R	Kuiper
2012-01-19	06:34 – 06:44	1.0871	0.1647	47.7	74.1	-36.2	19.0	3.0	60	R	Kuiper
2012-01-26	07:36 – 07:43	1.1078	0.1841	44.3	82.1	-31.4	19.2	2.8	30	R	Kuiper
2012-01-27	06:49 – 06:56	1.1107	0.1871	44.0	83.1	-30.7	19.2	2.8	60	R	Kuiper
2012-02-23	05:16 – 05:27	1.2016	0.3032	40.1	104.2	-15.4	20.3	1.9	60	R	Kuiper
2012-02-24	05:00 – 05:12	1.2051	0.3087	40.2	104.8	-15.0	20.4	1.9	60	R	Kuiper
2012-03-28	04:31 – 04:45	1.3233	0.5348	42.7	124.1	-5.2	21.8	1.5	60	R	Kuiper

Note: r and Δ are the distances of the asteroid from the Sun and the Earth, respectively, α is the solar phase angle, while λ and β are the geocentric, ecliptic (J2000) longitude and latitude. In the next column an average brightness V of the asteroid, as predicted by the Horizons ephemeris service, is given. Starting from the ninth column, the table gives the asteroid movement on the sky (Mov), the exposure time (Exp), and the filters used (the abbreviation *Spec* denotes spectroscopic observations)

presents one of the lightcurves obtained during our observations. It shows relative brightness variations of the asteroid in the Sloan r filter, and of one of the comparison SDSS stars. There are no traces of periodicity in these data with a peak-to-peak amplitude greater than 0.05 mag. The observed scatter is probably caused by imperfect flat fielding rather than statistical noise. Assuming that a typical asteroid displays a bimodal brightness variation we can conclude the rotation period of 2000 FJ₁₀ P is longer than twice the time span covered by our data ($P > 36$ min). The data obtained on another night with the r filter were analysed in the same way. As it also showed no discernible light variation, we can raise the lower limit for P to 94 min. Of course, there is a small probability that at the time of our observations the asteroid was visible close to the pole-on view and its brightness variations were difficult to detect – despite its short period.

Similar observations performed on 19 Oct with the Kuiper telescope revealed a systematic increase of the asteroid's brightness by ~ 0.3 mag during 37 min. This does not contradict our SALT observations as from 22 Sep to 19 Oct the solar phase angle almost doubled from 31° to 58° , while the observer-centred ecliptic latitude changed by 15° . This could have led to an increase of the lightcurve amplitude. It is also possible that our SALT observations were performed during maximum brightness, when the lightcurve for some time could be almost flat.

The fact that on 19 Oct during 37 min the asteroid lightcurve did not show any extremum can be used to raise further the lower limit for its rotation period from 94 min to about 2 hours (under the assumption of a typical bimodal lightcurve). We thus conclude that 2000 FJ₁₀ is not a fast rotator.

4.2. Taxonomy

From the photometric standpoint, an asteroid's taxonomy is usually determined from its colour indices in the Johnson UBVR system. Instead of transforming our Sloan g - r and r - i colours to their B - V and V - R counterparts we used an

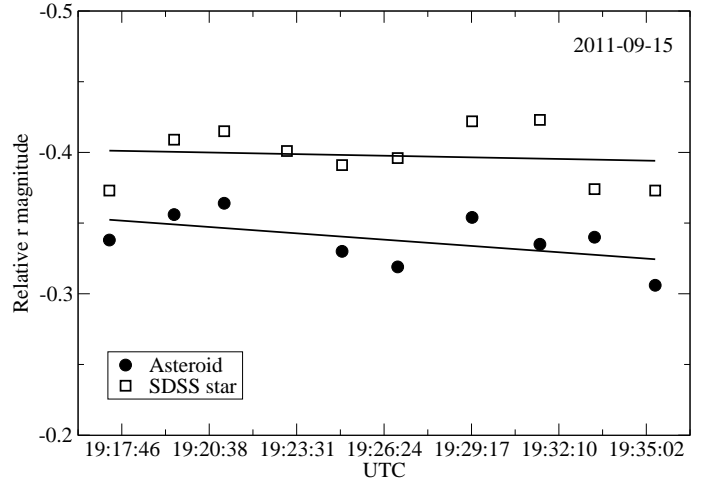


Fig. 2. Lightcurve of (190491) 2000 FJ₁₀ obtained in the Sloan r filter. There are no apparent periodic variations during 20 minutes with a peak-to-peak amplitude greater than 0.05 mag. The slope in the linear fit is too small to be significant. For comparison, brightness variations of one of the SDSS stars are also presented. The observed scatter of points is caused by the residual effects of the flat fielding procedure.

analogous classification based on the SDSS magnitudes. Ivezić et al. (2001) used 316 spectra obtained in the SMASS survey and convolved them with the SDSS response functions. As a result they were able to identify different taxonomic classes on the g - i vs r - i domain (Fig. 3). The position of 2000 FJ₁₀ on this graph shows it is most probably an S type, but V, D, or E, M, P types cannot be ruled out. This conclusion is supported by the $V - R = 0.48 \pm 0.05$ mag measured with the Kuiper telescope, which is consistent with an S-type classification (Tholen & Barucci 1989) and in agreement with the WHT spectrum.

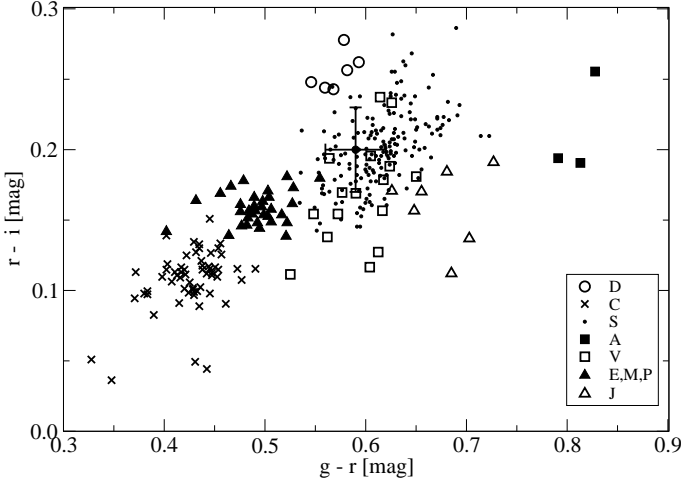


Fig. 3. Colour-colour plot for the 316 asteroids whose spectra were obtained by the SMASS Survey, based on Fig. 10 from Ivezić et al. (2001). Different taxonomic classes are presented by different symbols. The colours of 2000 FJ₁₀ (filled circle with error bars) are most compatible with an S type classification, though V, D or E, M, P types cannot be ruled out.

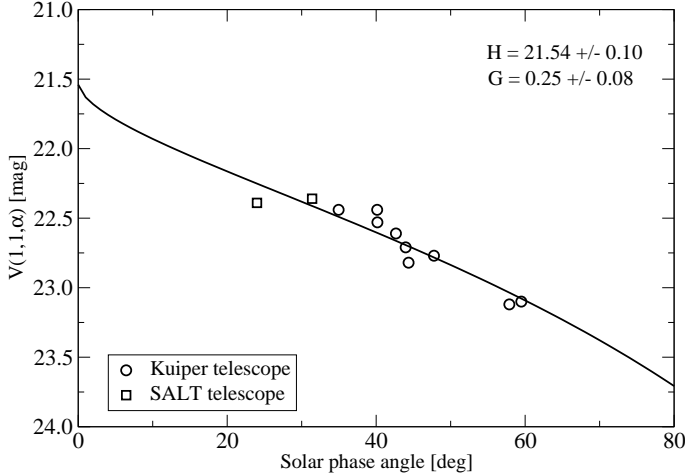


Fig. 4. Least-square fit of the H-G relation to the asteroid phase curve. The scatter of the points is partially caused by the changing aspect and the lightcurve amplitude.

4.3. Diameter

The observations of 2000 FJ₁₀ over a wide range of phase angles allowed us to plot its phase curve, and to derive the absolute magnitude as well as the effective diameter. The R magnitudes measured with the Kuiper telescope have been transformed to V magnitudes using its V-R colour index. The r magnitudes measured with SALT have been transformed to V magnitudes with the equations given by Jester et al. (2005) (for that we also used the asteroid $g-r$ colour index).

Figure 4 presents a plot of $V(1,1,\alpha)$ magnitudes versus solar phase angle. The apparent magnitude of the asteroid at each observation has been corrected to unit distance from the Sun and the Earth. A least square fit with the standard H-G relation (Bowell et al. 1989) gives $H = 21.54 \pm 0.10$ mag and $G = 0.25 \pm 0.08$. The quoted uncertainties were estimated by assuming error bars in

Table 2. (190491) 2000 FJ₁₀ clone classification statistics at different stages during the forward and backward integrations.

FORWARD				
Outcomes	time from integration start (yr)			
	$+10^4$	$+10^5$	$+5 \times 10^5$	$+10^6$
$q > 1.3$ AU	0	0	17	26
Amors	998	283	390	376
Apollos	1	705	486	425
Atens	0	11	106	172
BACKWARD				
Outcomes	time from integration start (yr)			
	-10^4	-10^5	-5×10^5	-10^6
$q > 1.3$ AU	0	1	5	18
Amors	996	979	667	569
Apollos	3	19	296	333
Atens	0	0	31	79

$V(1,1,\alpha)$ of ± 0.05 mag. It is worth noting the large discrepancy between $H = 20.9$ given by the MPC (based entirely on inaccurate magnitude estimates), and our result. It confirms a general rule that the MPC absolute magnitudes derived for NEAs are often underestimated by up to 0.5 mag.

The obtained value of $G = 0.25$ is consistent with the average value $G = 0.23$ obtained for S type asteroids (Lagerkvist & Magnusson 1990), further supporting our taxonomic classification of 2000 FJ₁₀ as an S type object.

Recently, improved albedo estimates for NEAs in different taxonomic classes were derived (Thomas et al. 2011). The average geometric albedo for the S complex was found to be $p_V = 0.26^{+0.04}_{-0.03}$. Using this value with our H magnitude, and the classic formula provided by Fowler & Chillemi (1992), we obtain for 2000 FJ₁₀ an effective diameter of $D_{\text{eff}} = 0.13 \pm 0.02$ km.

5. Dynamical Modelling

5.1. Method

To characterise the asteroid's recent orbital evolution and constrain its origin, we have generated 1000 dynamical clones of 190491 by applying the formal state covariance of that asteroid for Julian Date 2455600.5 downloaded from *AstDys*² to a six-dimensional gaussian random vector (see Duddy et al. 2012, for details). The clones were then integrated 10^6 yr in the past and in the future under an 8-planet model of the solar system. The integrations were carried out using the hybrid scheme which is part of the MERCURY package (Chambers 1999). This scheme is based on a second-order mixed variable symplectic (MVS) algorithm; it switches to a Bulirsch-Stoer scheme within a certain distance from a massive object. For all the integrations reported here, this distance was 2 Hill radii. The integration time step was chosen to be 4 days (1/20th of the orbital period of Mercury). During the integration, MERCURY detected and recorded close approaches with the terrestrial planets. We caution that, **despite** the time reversibility of the equations of motion in the absence of

² <http://hamilton.dm.unipi.it/astdys/>

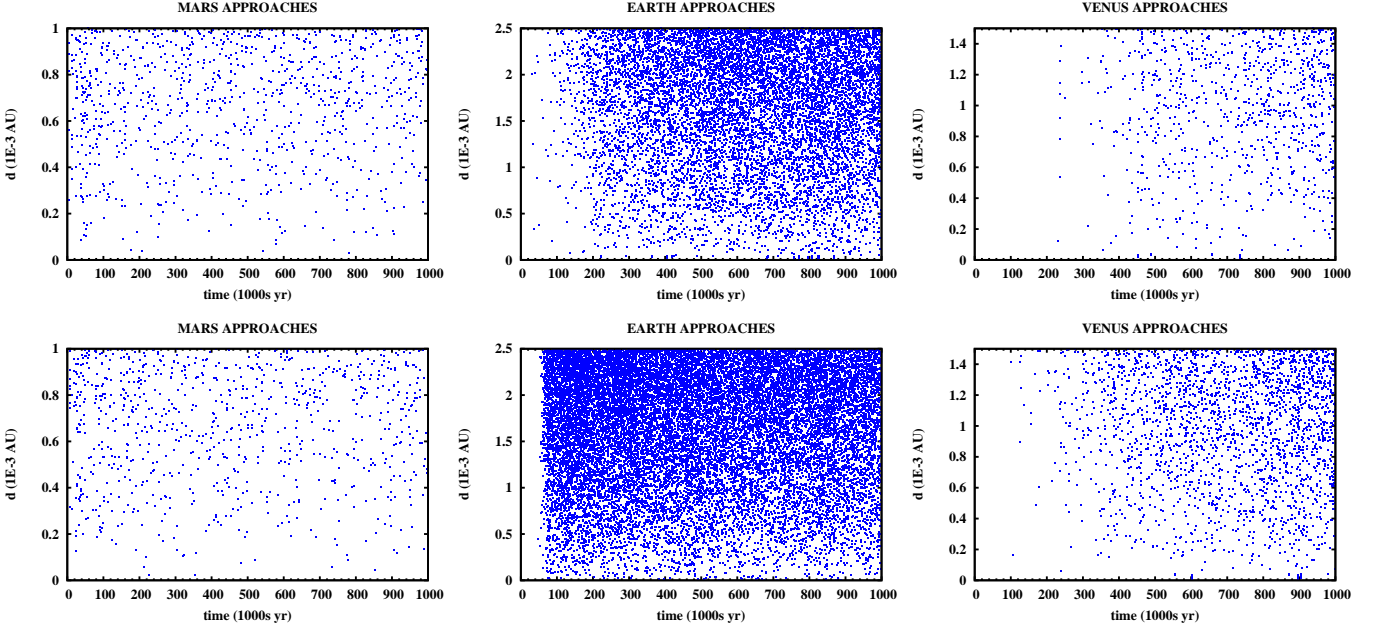


Fig. 5. Minimum distances during encounters with Mars (left), Earth (middle) and Venus (right) as recorded by MERCURY during the backward (top) and forward (bottom) integrations of 1000 clones of (190491) 2000 FJ₁₀.

dissipation, backwards integrations will not, in general, provide information of the dynamical history of the asteroid; instead, the forward evolution starting from the possible source regions must be considered (Bottke et al. 2002). As we show in the following, however, the case of (190491) 2000 FJ₁₀ can be considered exceptional in this sense. In addition, the Yarkovsky effect (Bottke et al. 2006) was not taken into account; we expect that its contribution to the dynamical evolution of the asteroid will be negligible compared to those of planetary close encounters and secular perturbations.

5.2. Dynamical Evolution

Figures 5, 6 and Table 2 show the distribution of the close approach distances of the clones to Mars, Earth and Venus as a function of time, the distributions of their perihelia and aphelia and their orbital classification statistics. Note that we have used the Minor Planet Center definitions for the Amor, Apollo and Aten NEA classifications. These are slightly different than those used by other authors (eg Bottke et al. 2002).

At present the clones of this Amor asteroid are experiencing close approaches with Mars but not with either Earth or Venus (left panels of Fig. 5). Despite the clones’ nominal perihelion distance being ~ 1.01 AU, this situation persists ± 10 kyr into the integrations. At that time, essentially all clones have $q > 1$ AU (left panels of Fig. 6) and remain classified as Amors (Table 2). One likely contributing factor is a 3:2 near-resonance between the orbital periods of 190491 and the Earth, which renders close encounters with the planet infrequent if not impossible (see Section 7).

In the backward integrations, close approaches of clones to the Earth occur at a gradually increasing rate (upper middle panel of Fig. 5) during a period of ~ 300 kyr. Their

perihelia remain at or above 1 AU at -100 kyr (upper middle panel of Fig. 6); consequently they retain their Amor classification (Table 2). By that time, only 15 clones have experienced close encounters with the Earth. In the forward integrations, the onset of Earth encounters is abrupt and occurs between $+50$ and $+100$ kyr. At $+100$ kyr most of the clones have perihelia < 1 AU and have become Apollos (lower middle panel of Fig. 6; Table 2). This difference between the outcomes of the forward and backward integrations is likely due to the secular evolution of the eccentricity. Fig. 7 shows the time series of a and $e \pm 2 \times 10^5$ yr from the present for one in every 20 clones. Although the evolution of individual clones is inherently chaotic, we note a statistical trend towards smaller values of e in the past and larger values of e in the future. The timescale of variation ($50+$ kyr) leads us to suspect that it is related to one or more of the secular eigenmodes of the solar system (Laskar 1990). The “critical” value of e required to reduce q below 1 AU is 0.25 for a mean a value of 1.33 AU. Once e increases past that critical value - indicated by the gray dashed line - in the forward integrations, Earth encounters become possible (see Fig. 5) and, as a result, the scatter in a and e (bottom panels) increases significantly. In the backward integrations, the critical value for e is never reached for all but a few cases.

This result likely reflects a predictable event of the asteroid’s dynamical evolution. In other words the real asteroid will begin encountering the Earth sometime in the interval 50-100 ky in the future and, as a consequence, become an Apollo asteroid.

The final orbital distribution of the clones is shown in the right panels of Fig. 6 and the last column of Table 2. Assuming Poissonian statistics (ie $\sigma = \sqrt{N}$), the asteroid is more likely to be an Amor than not an Amor ($3\text{-}\sigma$ level) at $t = -1$ Myr. In the forward integrations, we can make the weaker statement that the most likely out of the four possible outcomes we examined is an Apollo classification.

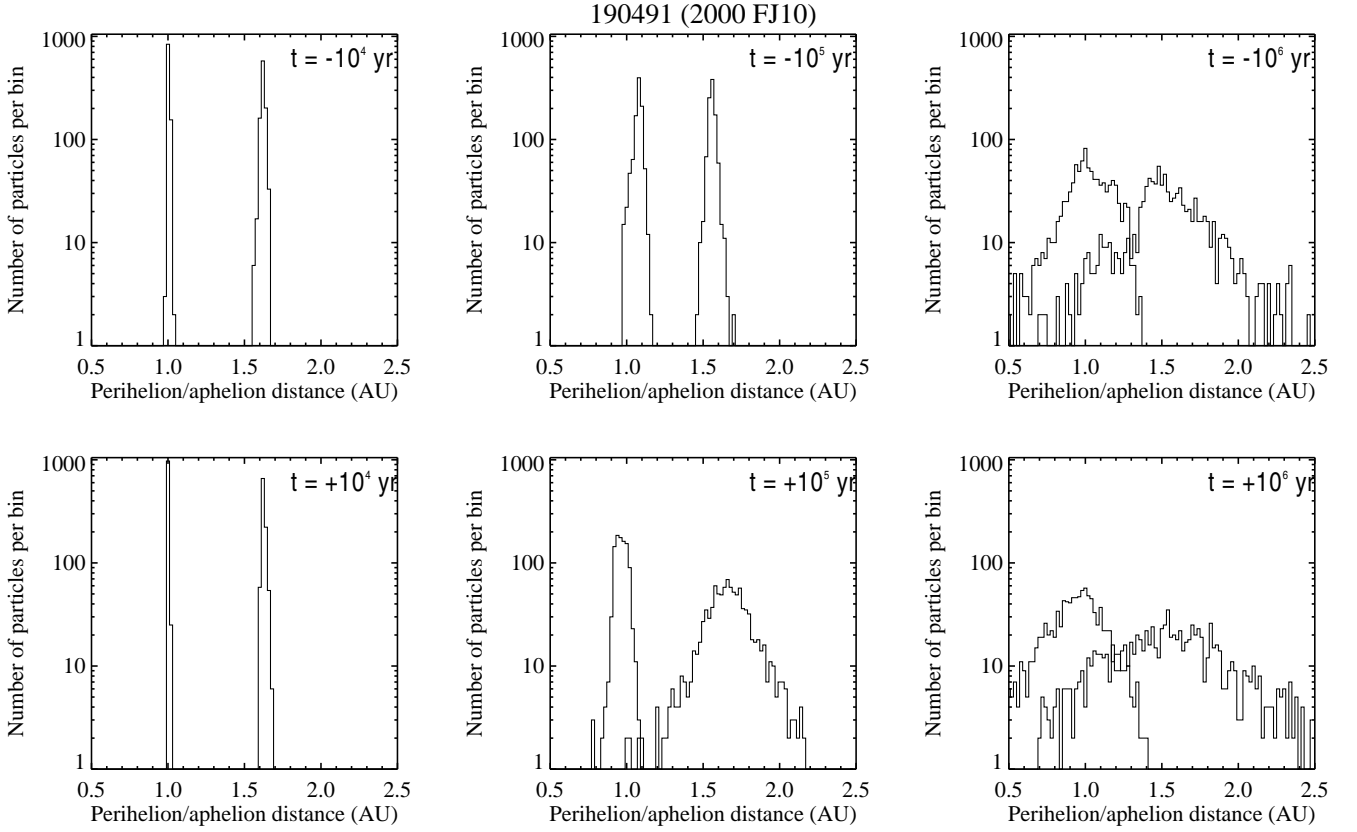


Fig. 6. Distribution of clone perihelion and aphelion distances of 1000 clones of (190491) 2000 FJ₁₀ at three different times during the backward (top) and forward (bottom) integrations.

However, this result is only significant at the 2- σ level when compared to that of an Amor classification. The final perihelia and aphelia of the clones appear to be more widely dispersed for the forward than for the backward integrations. Finally, we note that the forward integrations produced a significant fraction of Atens and that two of the clones collided with the Sun, a common end result of NEA dynamical evolution (Farinella et al. 1994).

5.3. Probability of collision with the Earth

The distribution of close approaches as a function of distance can be used to estimate the collision probability with the Earth. To do this, we first converted the recorded distances q_i and speeds v_i at closest approach to impact parameters b_i and velocities at infinity $v_{\infty,i}$ through the expressions (Öpik 1976):

$$v_{\infty,i} = \sqrt{v_i^2 - 2\mu/q_i} \quad (1)$$

$$b_i = q_i \sqrt{1 + \frac{2\mu}{q_i v_{\infty,i}^2}} \quad (2)$$

where μ denotes the product of the planet's mass with the gravitational constant G .

Then we collected the b_i into bins of width $\Delta b_i = 0.005$ in units of the Earth's Hill radius ($\simeq 0.01$ AU) and fitted linear laws to the data for the backward and forward integrations separately, expecting that

$$N(b_i) = N(b_i < b < b_i + \Delta b_i) \sim b_i \Delta b_i. \quad (3)$$

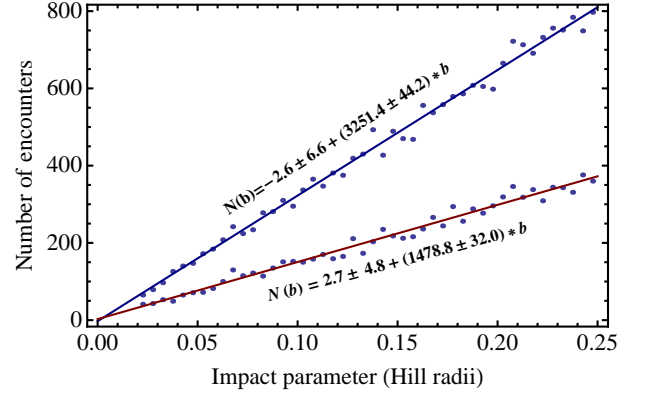


Fig. 8. Linear fit to the number of close encounters to the Earth as a function of the impact parameter b for the forward (upper curve) and the backward (lower curve) integrations.

Figure 8 shows that the frequency of deep close encounters ($\ll 1R_H$) is higher in the future than in the past, consistent with the higher dispersion of future over past clones as found earlier in this Section. The expected number of collisions with the Earth per Myr is $N_c = \int_0^{b_E} N(b)db$ where b_E is calculated from Eq. 2 by setting $q = R_E$, Earth's radius and assuming $v_{\infty,E} = \langle v_{\infty,i} \rangle \simeq 5.8 \text{ km s}^{-1}$. This evaluates to ~ 0.11 and ~ 0.08 for the forward and backward integrations respectively. Hence the probability of im-

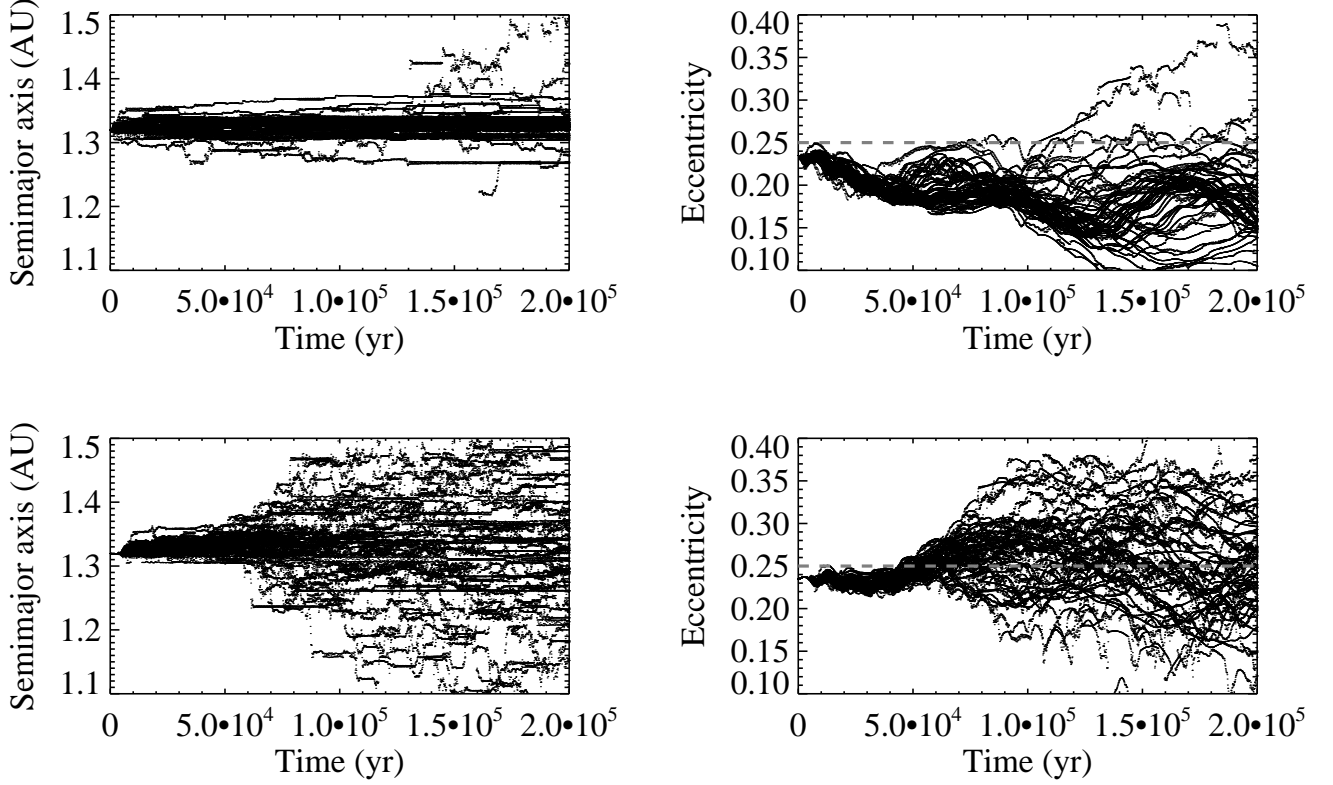


Fig. 7. Orbital evolution of asteroid clones 2×10^5 yr backwards (top) and forwards (bottom) from the present. The left panels show the semimajor axis while the right panels show the eccentricity. Only one in every twenty clones is plotted to maintain clarity. The grey dashed line denotes the minimum eccentricity required for an orbit with a semimajor axis of 1.33 AU to cross that of the Earth.

part of (190491) 2000 FJ₁₀ with the Earth in the interval $[-10^6, 10^6]$ yr is $\sim 2 \times 10^{-4}$.

6. Synthesis: The Origin of 2000 FJ₁₀

Bottke et al. (2002) found that $\sim 85\%$ of all NEOs with $H < 22$ originate in either the inner (IMB; $a < 2.5$ AU) or central (CMB; $2.5 \text{ AU} < a < 2.8$ AU) Main Belt. About half ($\sim 53\%$) of existing Amors originate in the inner Belt alone. They are delivered in the terrestrial planet region via the 3:1 mean motion resonance with Jupiter, the ν_6 secular resonance and close encounters with Mars (see also Binzel et al. 2004). The S-complex taxonomic classification deduced from our observations is consistent with this premise. The dynamical simulations show that it has been an Amor for at least 100 kyr from the present. The gradual loss of determinacy in the eccentricity evolution (Fig. 7) allows us to extend the validity of this statement for up to a few 100s of kyr in the past. Since only a few clones attained perihelia > 1.3 au at the end of both the forward and backward integrations, we conclude that, if it arrived from the asteroid belt, it likely did so > 1 Myr ago. A small but statistically significant difference between the outcomes of the full 1 Myr runs in the past and in the future suggests that the real asteroid is currently evolving from the Amor to the Apollo dynamical class. However, given the caveats in interpreting backwards integrations mentioned in Section 5.1, we believe this conclusion to be tentative. To better quantify the likelihood of different scenarios, it would be

necessary to apply methods such as that of Bottke et al. (2002).

We also note that $> 95\%$ of clones in both forward and backward integrations maintained an inclination of $< 15^\circ$, indicating that it is unlikely to have originated in the high inclination Hungaria and Phocaea families. If it originated within either the IMB or the CMB (source regions of 75% of Amors according to Bottke et al. 2002) it may be a former member of a family dominated by S-type asteroids, the most populous of which are the Flora and Eunomia families (Zappala et al. 1995).

7. Accessibility from the Earth

To quantify the accessibility of the asteroid from the Earth, we constructed two way (Earth - Asteroid - Earth) Type II keplerian arcs based on the Gauss method as in Bate et al. (1971). Arrival and departure dates were determined by minimising the ΔV at the asteroid. We considered that a launch/return window existed when this quantity was equal to or less than that expended by the NEAR spacecraft in 1999 to rendezvous with 433 Eros in early 2000 ($\sim 0.965 \text{ km s}^{-1}$; Dunham et al. 2002). We found that consecutive launch windows for the asteroid are spaced ~ 3 years apart (upper panel of Fig. 9) and that the same holds for return windows (lower panel of Fig. 9). Typical one-way trip times are ~ 1 year with a one-year wait at the asteroid before insertion into the Earth return trajectory.

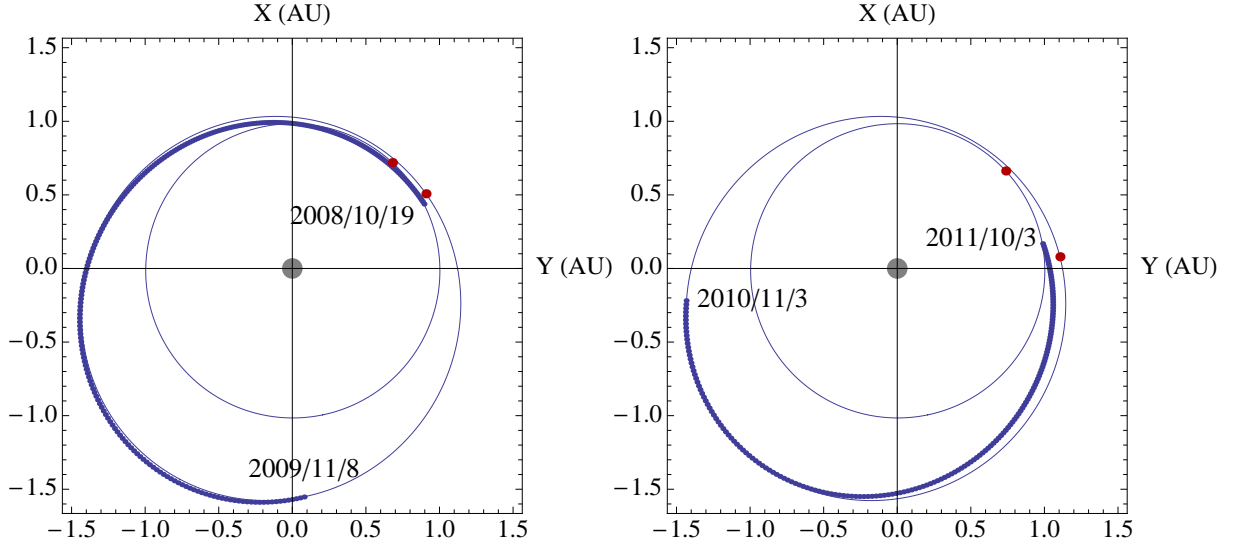


Fig. 10. Round trip to 190491 using Type II two-impulse transfers. Left: outbound leg. The locations of the asteroid at departure and the Earth at arrival are denoted by the red disks. Right: Return leg. The red disks now indicate the location of the Earth at departure and that of the asteroid at Earth arrival.

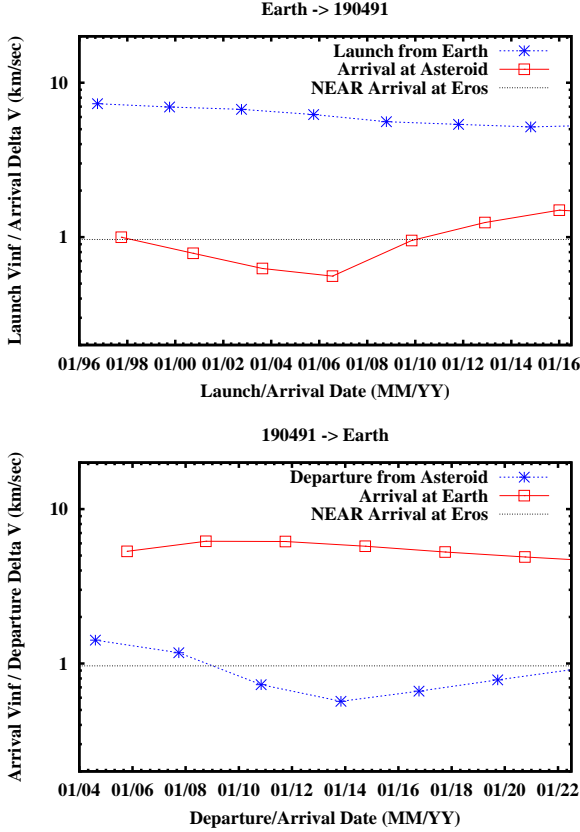


Fig. 9. Top: Departure v_∞ and ΔV required to match speeds with 190491 at arrival. The ΔV expended by NEAR upon arrival at 433 Eros is indicated. Bottom: Return leg.

A set of example trajectories generated by our code are shown in Fig. 10. Departure from Earth occurs in Autumn 2008 ($v_\infty = 5.5 \text{ km s}^{-1}$) and arrival the following Autumn ($\Delta V = 0.95 \text{ km s}^{-1}$). Departure one year later ($\Delta V = 0.75 \text{ km s}^{-1}$) brings the hypothetical spacecraft back to the Earth in October 2011 ($v_\infty = 6.3 \text{ km s}^{-1}$). It is important

to note for the discussion that follows that departure from and return to the Earth occurs when the asteroid is nearby.

Interestingly, during the period 2000-2100 AD favourable launch windows occur in two groups, the first in 2000-2012 and the second in 2047-2059. Corresponding favourable return windows span the periods 2010-2020 and 2058-2070 respectively. On those occasions rendezvous with the asteroid requires $< 1 \text{ km s}^{-1}$ of ΔV and a similar amount for departure and return to the Earth. The total ΔV for arrival at, and departure from, the asteroid is $< 2 \text{ km s}^{-1}$ on three round-trip opportunities in the period 2052-2061.

We find that this is the result of a 3:2 near-resonance between the orbital period of the asteroid and that of the Earth. This is best demonstrated if one views the asteroid's trajectory in a frame that rotates with the Earth's mean angular velocity around the Sun (Fig. 11). Due to the near-resonance the asteroid traces out a pattern with respect to the Earth completing one revolution every 3 Earth years (left panel). The two loops correspond to the asteroid passing through the pericentre of its orbit. As of 2011 (left panel), one of those loops lies close to the Earth. Because the resonance is not exact, the pattern slowly precesses in a clockwise direction so that, after 15 years (i.e. 2026) close approaches to the Earth are no longer possible (middle panel). Half a precession period later (18,000 d or 50 yr) the original configuration is recovered and close approaches to the Earth become possible again (right panel). In fact, querying the asteroid's ephemeris using the MPC online tool³ shows that the two closest approaches of the asteroid to the Earth ($\Delta \simeq 0.1 \text{ AU}$) for the remainder of the 21st century occur in 2058 and 2061.

8. Conclusions

The Amor NEA (190491) 2000 FJ₁₀ is one of the most accessible spacecraft targets. Its effective diameter of $D_{\text{eff}} = 0.13 \pm 0.02 \text{ km}$ places it in the transition zone between grav-

³ <http://www.minorplanetcenter.net/iau/MPEph/MPEph.html>

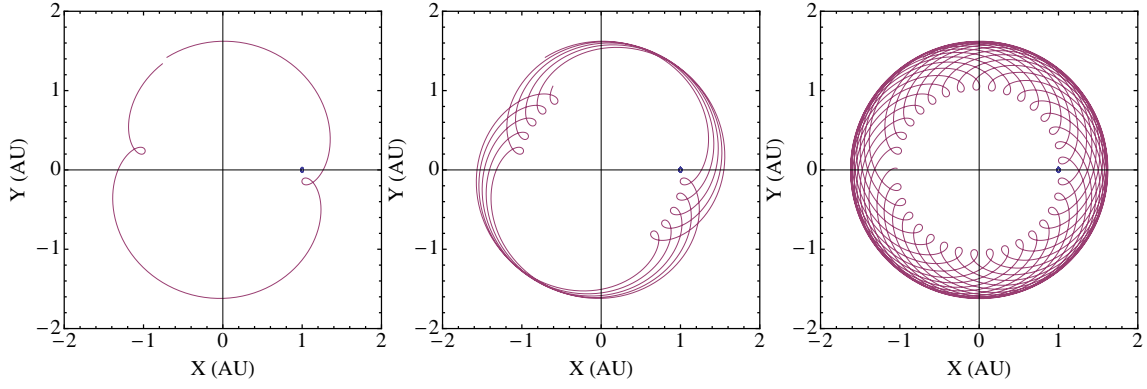


Fig. 11. The trajectory of the asteroid in a frame rotating with the Earth's mean motion over periods of 3yr (left panel), 15 yr (middle panel) and 50 yr (right panel). The small ellipse at (1,0) represents the trajectory of the Earth in this frame, due to its orbital eccentricity (~ 0.017).

itationally bound rubble-piles and monolithic bodies, held together by their internal strength (Asphaug et al. 2002).

2000 FJ₁₀ belongs to the S-complex of evolved asteroids, making it scientifically less interesting than the primitive objects that are usually the targets of robotic sample-return missions. On the other hand, its relatively large size, slow rotation, and accessibility from the Earth can make it a source of minerals and elements important for industry and a suitable target for a piloted mission (Abell et al. 2009).

Due to its Earth-like orbit, during the next 10 years 2000 FJ₁₀ will make several close approaches to the Earth which can be used to determine its shape and spin axis orientation. Until 2020, there will be favourable apparitions of decreasing quality every 3 years when the asteroid will be brighter than $V = 21$ mag. This is rather uncommon among NEAs.

Acknowledgements. Astronomical research at the Armagh Observatory is funded by the Northern Ireland Department of Culture, Arts and Leisure (DCAL). TK and MB were supported by the Narodowe Centrum Nauki grant N N203 403739. The authors wish to acknowledge the SFI/HEA Irish Centre for High-End Computing (ICHEC) for the provision of computational facilities and support. Based on observations made with the William Herschel Telescope operated on the island of La Palma by the Isaac Newton Group in the Spanish Observatorio del Roque de los Muchachos of the Instituto de Astrofísica de Canarias. Some of the observations reported in this paper were obtained with the Southern African Large Telescope (SALT). A. G. acknowledges support from the National Research Foundation (NRF) of South Africa.

References

Abell, P., Korsmeyer, D. J., Landis, R. R., et al. 2009, *M&PS*, 44, 1825
 Asphaug, E., Ryan, E. V., & Zuber, M. T. 2002, *Asteroids III*, 463
 Bate, R. R., Mueller, D. D., & White, J. E. 1971, *Fundamentals of Astrodynamics* (Dover Publications, New York)
 Binzel, R. B., Rivkin, A. S., Stuart, J. S., et al. 2004, *Icarus*, 170, 259
 Bottke, W. F., Morbidelli, A., Jedicke, R., et al. 2002, *Icarus*, 156, 399
 Bottke, W. F., Vokrouhlický, D., Rubincam, D. P., & Nesvorný, D. 2006, *Ann. Rev. Earth Planet. Sci.*, 34, 157
 Bowell, E., Hapke, B., Domingue, K., et al. 1989, In: *Asteroids II* (Binzel, R. P. and Gehrels, T. and Matthews, M. S., Eds), University of Arizona Press, Tucson, 524
 Bus, S. J. & Binzel, R. P. 2002, *Icarus*, 158, 106
 Chambers, J. E. 1999, *MNRAS*, 304, 793
 Crawford, S. M., Still, M., Schellart, P., et al. 2010, in *Society of Photo-Optical Instrumentation Engineers (SPIE) Conference Series*, Vol. 7737, Society of Photo-Optical Instrumentation Engineers (SPIE) Conference Series

DeMeo, F. E., Binzel, R. P., Slivan, S. M., & Bus, S. J. 2009, *Icarus*, 202, 160
 Duddy, S. R., Lowry, S. S., Wolters, S. D., et al. 2012, *A&A*, 539, A36
 Dunham, D. W., McAdams, J. V., & Farquhar, R. W. 2002, *APL Tech. Digest*, 23, 18
 Elvis, M., McDowell, J., Hoffman, J. A., & Binzel, R. P. 2011, *P&SS*, 59, 1408
 Farinella, P., Froeschle, C., Froeschle, C., et al. 1994, *Nature*, 371, 315
 Fowler, J. W. & Chillemi, J. 1992, in *The IRAS Minor Planet Survey*, ed. E. Tedesco, G. Veeder, J. Fowler, & J. Chillemi (Phillips Laboratory, Hanscom Air Force Base, MA), 17–43
 Hasegawa, S., Müller, T. G., Kawakami, K., et al. 2008, *PASJ*, 60, S399
 Hergenrother, C. W. & Whiteley, R. J. 2011, *Icarus*, 214, 194
 Horne, K. 1986, *PASP*, 98, 609
 Ivezić, Ž., Tabachnik, S., Rafikov, R., et al. 2001, *AJ*, 122, 2749
 Jester, S., Schneider, D. P., Richards, G. T., et al. 2005, *AJ*, 130, 873
 King, D. L. 1985, *La Palma Technical Note 31*
 Kniazev, A. & Väisänen, P. 2011, *SALT Technical Note 2251AC0001*
 Kwiatkowski, T., Buckley, D. A. H., O'Donoghue, D., et al. 2010, *A&A*, 509, A94
 Lagerkvist, C.-I. & Magnusson, P. 1990, *A&AS*, 86, 119
 Landolt, A. U. 1992, *AJ*, 104, 340
 Laskar, J. 1990, *Icarus*, 88, 266
 Lauretta, D. S., Drake, M. J., Binzel, R. P., et al. 2010, *M&PSA*, 73, 5153
 Michel, P., Barucci, A., Koschny, D., et al. 2009, *M&PSA*, 72, 5261
 O'Donoghue, D. E., Bauermeister, E., Carter, D. B., et al. 2003, *Proc. SPIE*, 4841, 465
 Öpik, E. J. 1976, *Interplanetary Encounters: close range gravitational interactions* (Elsevier, Amsterdam)
 Tholen, D. J. & Barucci, M. A. 1989, in *Asteroids II*, ed. R. P. Binzel, T. Gehrels, & M. S. Matthews (University of Arizona Press, Tucson), 298–315
 Thomas, C. A., Trilling, D. E., Emery, J. P., et al. 2011, *AJ*, 142, 85
 Zappala, Z., Bendjoya, P., Cellino, A., Farinella, P., & Froeschle, C. 1995, *Icarus*, 116, 291